Comparative Assessment of Wearable Surface EMG Electrode Configurations for Biomechanical Applications

J. Walter Lee[1], Alireza Golgouneh[2], *and* Lucy Dunne[3]
Wearable Technology Lab, University of Minnesota – Twin Cities, St. Paul, MN, 55108

Obtaining accurate biomechanical information within rigid, constrained compartments such as spacesuits can be challenging and labor-intensive, due to the obstacles of bulk and mass involved with sensor placements. Inspired by the current challenges in measuring astronaut biomechanics and in designing mobility-assistive robotics, this study investigates the feasibility of using soft, flexible wearable surface electromyography (EMG) sensors. In this study, anti-slip arm bands with textile-friendly metal-snap electrodes were used to collect EMG signals from biceps brachii and triceps brachii muscle activities, with conventional adhesive disposable solid-gel electrodes measuring the same muscle activities simultaneously. To compare the quality of signals obtained from the wearable EMG electrode configuration to the signals obtained from the conventional EMG electrodes, 40 trials that were collected with two subjects were analyzed by extracting 11 time-domain EMG features. These EMG features from two distinct signal sources were compared by using the non-segmentation method, the overlapping segmentation method, and the disjoint segmentation method. Results showed that comparisons were non-significant in most feature comparisons using non-segmentation method, and all comparisons were non-significant in both EMG signal segmentation methods, validating the feasibility of reliable and accurate signal collection with the dry metal-snap wearable electrodes and the promise in real-time application of the wearable EMG electrode configuration. Implications and limitations of the current study results are also discussed.

Nomenclature

AC	=	alternating current
Ag-AgCl	=	silver-silver chloride
AR	=	autoregressive
CMRR	=	common-mode rejection ratio
DAMV	=	difference absolute mean value
EMG	=	electromyography
EVA	=	extravehicular activities
IEMG	=	integrated absolute value of EMG
k	=	time index of EMG signal
MAV	=	mean-absolute-value
MVC	=	maximum voluntary contraction
NBL	=	Neutral Buoyancy Laboratory
N.S.	=	non-significant
RMS	=	root-mean-sqaure
sEMG	=	surface electromyography
SSC	=	slope sign change
SD	=	standard deviation
WL	=	wave length
VAR	=	variance
WAMP	=	Wilson ampitude
ZC	=	zero crossings

[1] M.S. Student / Research Assistant, Human Factors and Ergonomics, College of Design, 240 McNeal Hall, University of Minnesota – Twin Cities, St. Paul, MN 55108.
[2] Ph.D. Student / Research Assistant, Department of Electrical Engineering, 240 McNeal Hall, University of Minnesota – Twin Cities, St. Paul, MN 55108
[3] Associate Professor, Department of Design, Housing, and Apparel, College of Design, 240 McNeal Hall, University of Minnesota – Twin Cities, St. Paul, MN 55108.

I. Introduction

The collection of biomechanical variables from human bodies moving within a rigid wearable hardware such as gas-pressurized spacesuits or mobility-assistive robotic exoskeletons presents unique challenges for researchers. Of particular relevance for aerospace concerns the frequent musculoskeletal injuries occurring to suited astronauts, during extravehicular activities (EVA) as well as during simulated training in the Neutral Buoyancy Laboratory (NBL).[1,2] It is believed that having to exert straining forces while maneuvering inside rigid spacesuits contributes to these injury occurrences.[3] However, it has been difficult to measure and characterize the exact body movements inside spacesuits that lead to such injuries. Due to the thick, rigid shell of the suit surrounding the body, accurate measurement of real-time body movements inside spacesuits with dynamic imaging techniques has not been useful. Injury preventation strategies for suited astronaut activities based on anecdotes, opinions, and static imaging results, therefore have not been fully effective.[1,4]

Beyond the need for designing astronaut injury prevention strategies, accurate measurement of biomechanics has also been important for the development of wearable mobility assistive devices, such as robotic exoskeletons for neuromuscular disorder rehabilitation and human strength augmentation in extreme environments.[5,6] Research efforts in the last two decades have yielded inventions including rehabilitative robotic suits and strength-augmenting exoskeletons for military and industry applications. However, many if not most of the current systems are constructed with rigid hardware, which may fundamentally compromise user mobility and comfort, or may induce stress on the machine.[7] Flexible actuation technologies are being researched in the new paradigm of soft robotics,[7–11] but there also remains a great need for a comfortable and wearable biomechanical sensing method to control mobility assistive systems. Being able to accurately and reliably quantify human biomechanics with a comfortable and flexible sensing technique therefore may be not only useful in building a control system for future generations of mobility assistive robotic devices, but also helpful for planning astronaut injury prevention strategies and designing more ergonomic spacesuits that lead to fewer injuries.

A classical approach for biomechanical analysis involves gathering goniometric information (joint angles) or sensing the force/torque between the body and the mechanical components.[12] However, such input variables provide limited information, due to the inherent blindness for user intent. Not all muscle activations produce actual joint motion (as in the case of isometric muscle contractions); conversely, passive body motions from external forces may be erroneously registered as intended movements. Such information about unobserved muscle activities or unintended motions cannot be effectively obtained with goniometers, inertial sensors, or force/pressure meters alone. Consequently, there are disadvantages to using such mechanical input variables in mobility assistive devices for rehabilitation or strength augmentation applications, because the user may not always possess sufficient muscle strength to produce detectable joint motion, and passive movements from external sources may trigger unintended actuations that threaten the safety of user and/or other individuals.

One alternative method for obtaining user biomechanical data is electromyography (EMG), which can provide unique information about the user's intended movements with the electrical signals that correspond to the sequence, duration, and magnitude of muscle fiber activations. Although subcutaneous needle electrodes may be used in clinical settings, surface electromyography (sEMG) with on-skin electrodes is the most common and recommended EMG signal collection approach due to its non-invasiveness. sEMG is not only widely used in kinesiological research involving the acvitities of superficial muscles, but also being used in many rehabilitative orthoses/prostheses designs due to the advantages of being able to detect muscle activation signals irrespective of actual joint motions. Even without sufficient joint torque produced by the user, researchers are able to detect the contractive efforts generated by the user's muscles, and such signals can also be used to control assistive robotics to correspond to the user-intended motions.[13] Also, EMG-based kinetic estimation methods do not require inverse dynamic modeling of the interaction between the body and the environment, bypassing the need for a priori knowledge of mass and inertia of body segments that may not be accessible in the wild.[14,15]

However, obtaining sEMG signals within rigid wearable compartments is challenging, and there are several drawbacks to collecting sEMG signals within spacesuits or robotic mobility assistive systems in terms of applicability and efficiency. Electrodes and wires required for the data collection are bulky and movement-restrictive; the adhesives and conductive gels used with disposable electrodes are time-consuming and labor-intensive to apply and may also cause discomfort or skin irriations.[16] The flimsy nature of sEMG signals also invites various noise issues such as the skin impedance between the target muscle and the electrode surface, slippage of the electrode against the skin, and motion artifact from wire friction or tugging.[17] Other electrode types with 'dry' surfaces are difficult to secure on body, suffering from relatively more signal noise and artifacts.[18] Cutting-edge wireless signal collection electrodes do not require cables, but their rigid supporting hardware typically does not fit comfortably underneath other systems and

may not transmit quality signals through the thick wearable shell and large environments like NBL. Therefore, despite the advantages of utilizing EMG signals for biomechanical studies and for assistive device control algorithms, the difficulties associated with signal collection have limited the feasibility of using EMG in many of these situations outside laboratory settings.[14] There is hence generally a great need for more compact, system-embedded, and easy-to-use electrodes across diverse applications.[19]

In this paper, we propose and validate an alternative method of collecting sEMG signals with a flexible, wearable physical interface that is easy to construct and does not necessitate individual electrode setups. We compare the features of the signals obtained from this wearable configuration to the those collected from conventional disposable electrodes. Several time-domain EMG features were chosen for this comparative analysis between the conventional and wearable EMG configurations, in order to assess the suitability of using this alternative flexible sEMG signal collection method in biomechanical studies and biomechatronics designs.

II. Background

A. Overview of Electromyography

1. Signal collection

The depolarized action potential waves that travel down along the muscle fibers upon excitation by the motor neurons are recorded during EMG sessions.[20] Depending on the intensity and duration of muscle activities, the frequency of muscle fiber innervation and the number of activated motor units may differ.[20] To capture such differences in the action potentials along their traveling routes, differential amplification with two electrodes per muscle are the standard configurations most commonly used.[20–22]

The gold standard sEMG procedure entails proper skin preparation with the removal of hair and/or dead skin cells to minimize the skin's electric impedance between the target muscle and the electrode surfaces.[22] On the target muscle, two electrodes are placed about 2 cm apart from each other along the belly of the muscle; it is best to avoid placing electrodes directly on or near the innervation zone or the insertion tendon.[21,23] Another electrode is used as the reference for canceling out the common signal noise, often placed on a bony prominence.[23]

The normal EMG signal has amplitude ranges of 0-10 mV peak-to-peak, and the frequency ranges of 0-500 Hz with most frequencies in the 50-150 Hz window.[23] To achieve good signal quality, a band-pass filter is usually required during or after recording, with a high-pass filter removing the low-frequency noise (e.g., sensor drift, temperature changes, etc.) and a low-pass filter removing the high-frequency noise (e.g., radio signals, computers, etc.).[22] Because the raw EMG signals are very weak, the signal should also be amplified accordingly; with passive cables usually a gain of at least 1000 is recommended.[22,24]

In addition, the EMG signals need to be 'normalized' in many cases, because the absolute signal amplitude can vary strongly across electrode placements, different EMG sessions, and different subjects.[24] Often the maximum voluntary contraction (MVC) values are collected to determine the reference point of the '100%' muscle strength exertion, by making the subject push or pull an immovable object, or the maximum amplitude from a single session may also be used for normalization if collecting MVC values is not feasible.[21] Normalization is nonetheless important for comparing across different individuals and different EMG sessions that have different signal means and ranges.[21] Lastly, further signal processing is necessary depending on the amount of collected noise and the exact test objective and collected noise level, to convert signals into cleaner forms for analysis; rectification, root-mean-square (RMS) processing, mean-absolute-value (MAV) processing are commonly used filtering/smoothing techniques; researchers may also choose to adapt advanced processing techniques such as whitening, demodulation, and relinearization.[17]

2. sEMG Electrode Types

Unlike the invasive needle electrodes used in intramusclular EMG, surface EMG electrodes are widely used with no required medical training and easier application. sEMG electrodes can be largely considered either gelled and dry, depending on the use of conductive gel.

- Gelled ("wet") electrodes require using a conductive electrolytic gel to form a layer of ion concentration gradient that works as a half-cell between the skin and the detecting electrode surface.[25,26] Silver-silver chloride (Ag-AgCl) is the most common electrode material to be used with the gel, due to its low resistance drift, low electrode-skin impedance, low noise, and low motion artifact.[27,28] Most Ag-AgCl electrodes are usually meant for one-time use and are hence disposable.[22]
- Solid gel electrodes work just like gelled electrodes, except for using polymerized jelly-like hydrogel substances instead of using the liquid gel.[29] Hydrogels are water-insoluble but also simultaneously hydrophilic, as they are composed of crosslinked three-dimensional polymer chains that hold water.[29,30] Hydrogel electrodes tend to have

slightly higher impedance than the liquid-gel electrodes, but are also simpler to apply, inexpensive, flexible, and sometimes reusable.[29–31]

- Dry electrodes such as bar electrodes or array/grid electrodes do not require any gel application between the skin and the electrode.[22] The lack of stabilizing electrolytic layer between the skin and the electrode surface means that the skin-electrode impedance is naturally higher and the electrode contact area is unstable. The ion concentration between the skin and the electrode surface is hence much more susceptible to external disturbances such as pressure and motion, leading to motion artifacts and signal noise.[25]
- Some electrodes, mainly dry electrodes, are active electrodes with built-in amplifiers, which can reduce cable motion artifact by amplifying the raw signals before being transmitted along the lead cables.[17,22] The presence of amplifier on/near the skin, however, entails encasing the electrode surfaces with hardware components for amplification, which may entail more bulk and mass that can be tricky to stabilize on the body. Conversely, the more commonly used electrodes that do not have built-in amplifiers are passive electrodes.

3. Common sEMG signal noise issues

- Skin impedance: Between target muscle fibers and electrode surfaces, the skin is a barrier in the sEMG signal collection. Generally, the thicker the skin and the subcutaneous tissues are, the higher the skin impedance will be, and the smaller the resulting sEMG signal amplitude will be.[21] Natrually the individual differences in the thickness of the skin may result in the variation in the sEMG amplitudes collected.[21]
- Unstable skin-electrode contact: sEMG data collection relies upon the contact between the electrode surfaces and the skin at the site of the target muscle. As mentioned, gelled electrodes offer the advantage of electrolytic layer that stabilizes the skin-electrode interface, with the formation of half-cell potentials across the electrode contact area.[25] Dry electrodes, with the lack of an electrolytic layer, electrode-skin impedance is higher and the contact stability is easily disturbed.
- Cable interference: The passive cables that relay the raw signals from the electrodes to the amplifier can easily pick up noise from ambient electromagnetic fields in the environment, if the cables are unshielded. It is recommended to use shielded wires to reduce such unwanted capacitances, but friction and deformation of the cable may still cause motion artifact with shielded wires.[17] As mentioned, active electrodes that have a built-in operational amplifier may significantly reduce cable interference; although the presence of amplifier requires additional housing for hardware.
- Alternating current (AC) power line interference: The AC power lines and the connected electric equipment have ambient electromagnetic fields; 60 Hz in North America and 50 Hz in Europe.[17] This power line interference needs to be minimized by shielding EMG data acquisition devices, and also can be removed by fixed notch filtering.[17] Proper electrode setup with the use of modern high-quality amplifier devices can normally prevent AC power line intereferences.[21]
- Motion artifact: Perhaps the biggest issue with most sEMG sessions is the motion artifact, caused by either (a) migration of the electrode on the skin, (b) skin deformation beneath the electrodes, or (c) cable friction and deformation.[17] To prevent motion artifacts, conductive gel is applied to stabilize the skin-electrode conduction, and sEMG electrodes and cables are often secured with additional tapes.[32] Such workarounds are commonplace but are not always robust against large physical movements, perspiration, or external disturbances. High-pass filtering may be necessary to reduce motion artifact collection.[23]

B. Wearable EMG Garment Prototype

Previous work by the first author involved designing a proof-of-concept prototype of a textile-based wearable interface that can measure EMG signals with garment-integrated dry electrodes (Figure 1).[33] This project was inspired by the difficulties in studying astronaut biomechanics that lead to injuries while carrying out suited EVA activities. The objective was to demonstrate the feasibility of collecting EMG data with a form-fitting garment that is reusable, washable, and does not involve time-consuming individual electrode setup for data collection.

Figure 1. Wearable EMG garment prototype.

With considerations on the easy-to-use form factor that allows reliable mechanical coupling of electrodes, many electrode materials and coupling methods were tested during the pilot testing stage of the project (Figure 3). Surprisingly, metal snaps with elastic wrapping around the limb worked well as sEMG electrodes with qualitatively good results. The final garment design consisted of form-fitting ponte roma knit fabric base with sewn-on pieces of Fabrifoam® medical compression wraps that offer elasticity, breathability, washability, and high resistance to on-skin migration (Figure 2). Metal snaps that work as electrode surfaces were attached onto these Fabrifoam® pieces, which were thereby secured on the skin without using any adhesive materials. The advantages of using metal snaps in this design included minimal electrical resistance, small size, easiness of repair, and accessibility.

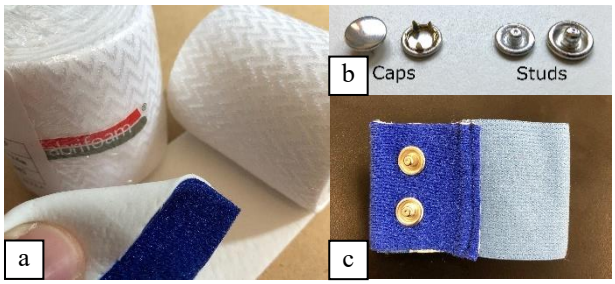

Figure 2. (a) Fabrifoam wraps; (b) Metal snaps; (c) sEMG electrode armband constructed with both materials and an elastic band.

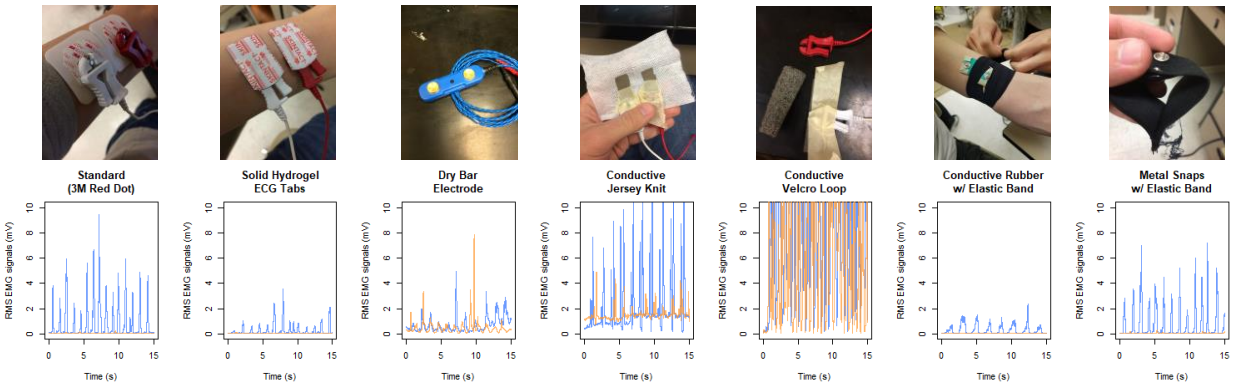

Figure 3. Selected examples of pilot-tested electrode configurations for the EMG garment design. Active biceps brachii flexion signals (blue) were compared with motion artifacts from externally created passive motions (orange). (RMS windows = 100 ms; sampling rate = 2 kHz)

The feasibility of using this wearable interface for EMG collection was also demonstrated with a human subject testing, where the garment showed qualitatively comparable signals as those obtained from conventional disposable electrodes (Figure 4). However, this demonstration was done with only one subject, and the direct quantitative comparison of the quality of EMG signals between the two methods was impossible, because the two methods did not collect the same muscle activities simultaneously. (Signals were first collected with conventional EMG electrodes, and then with the garment.) It is currently unclear how this simple method of securing dry metal snaps onto the skin with anti-slip medical wraps can perform as an acceptable way of collecting accurate, reliable EMG signals. Therefore, it is necessary to conduct feature-by-feature comparison of the EMG signals collected simultaneously on the same muscle with these two methods, as is done in the current study.

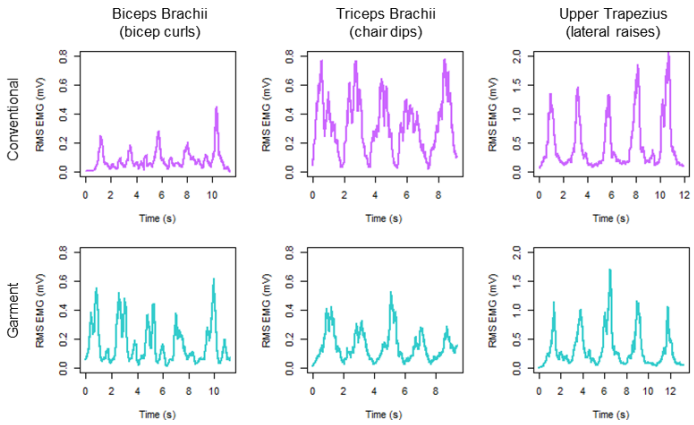

Figure 4. Example trials from the human subject testing of the EMG garment prototype. (Conventional = 3M Red Dot 2560 electrodes; RMS windows = 100 ms; sampling rate = 2 kHz)

III. Methods

A. Devices

1. Hardware and software equipment

All EMG signals were collected with a Biopac MP 160 system (Biopac Systems Inc., USA) and Biopac AcqKnowledge 4 software, with two EMG100C modules for recording two EMG channels simultaneously. The EMG signals were digitized with a sampling rate of 2 kHz, with a built-in notch filter of 60 Hz to cancel out the AC power interference. Both EMG channels also underwent a low-pass filter of 5000 Hz and a high-pass filter of 1 Hz during recording. The gain was set at 2000. The common-mode rejection ration (CMRR) was 110 dB min.

2. Dual-channel sEMG signal collection apparatus

Measuring two channels of sEMG signals simultaneously from the same muscle requires an unusual setup, with both the wearable sEMG recording method and the conventional sEMG recording method accurately implemented into a limited real estate. As mentioned, an ideal EMG setup requires two electrodes per channel to be placed on the center line of the muscle belly, but a simultaneous recording of two electrode pairs on the same muscle requires an unconventional electrode configuration of both signal collection methods.

To attach both pairs of electrodes on the same muscle, an adjustable armband-like apparatus with a Fabrifoam® piece was constructed (Figure 5). A piece of Fabrifoam® SuperWrap was cut off into a 3.75" × 3" rectangle, and a strip of elastic band was sewn on one end of it. Two metal snap electrodes were attached towards the middle of the the Fabrifoam® piece with an inter-electrode distance of 1 inch (center-to-center). Two holes were cut in a slightly oblong shape (0.75" × 0.5") about half-inch next to the metal snap electrodes, so that conventional adhesive electrodes can be attached alongside them with their studs exposed. The armband was closed with hook-and-loop strips, since Fabrifoam® products are Velcro-receptive; a small loop-side strip was sewn on the other end of the elastic band, and the armband was fastened on the arm with a hook-side strip on the other end.

Figure 5. Construction of armband for dual-channel sEMG signal collection of the same arm muscle.

B. Procedure

Two healthy male subjects performed the exercises analyzed in this study. Each subject donned the sEMG signal collection armband for each of the four arm muscles measured for comparison. As seen in Figure 6a, for each muscle, two Covidien H124SG electrodes (Ag-AgCl with solid gel) were chosen to be used as conventional adhesive electrodes, due to their small size (Ø 24 mm). These adhesive electrodes were applied on the muscle with an inter-electrode distance of approximately 1 inch. Adjacently on the same muscle belly, the two metal snap electrodes were placed and the armband was tightened with hook-and-loop strips, with the oblong holes on the Fabrifoam revealing conventional H124SG electrode studs (Figure 6b). Shielded clip-lead wires (Biopac LEAD110 series) were attached to these electrodes to connect to the Biopac MP160 system and EMG100C modules (Figure 6c). In addition, two 3M Red Dot 2560 electrodes (Ag-AgCl with solid gel) were applied on C7 spinal cord as reference electrodes (Figure 6d).

Figure 6. Testing procedure with the armband.

Then the subject performed the following exercises (Figure 6e). For the left biceps brachii and the right biceps brachii muscles, each subject performed 1 MVC trial (5 reps of maximum contraction) followed by 5 trials of dumbbell bicep curls (5 reps per trial, with either a 5-lb. or a 8-lb. dumbbell). Similarly, for the left triceps brachii and the right triceps brachii muscles, 1 MVC trial (5 reps of maximum contraction) was followed by 5 trials of overhead dumbbell tricep curls (5 reps per trial, with either a 5-lb. or a 8-lb. dumbbell). MVC trials involved trying to flex the extended arm while being pushed down (for the biceps brachii muscle) and extending the arm against an immovable wall (for the triceps brachii muscle). All conventional and wearable electrodes remained donned while all were trials collected from each muscle. Speed of the reps were subjectively controlled by the subject, with each trial lasting about 20-30 seconds. Subjects were allowed brief breaks in between trials and before switching to different muscles.

C. Data Analysis

1. Signal Standardization

Prior to the data processing, the signals obtained from the conventional and new electrodes were standardized by subtracting the difference between their means and scaling their amplitudes onto [-1 and +1] (Figure 7).

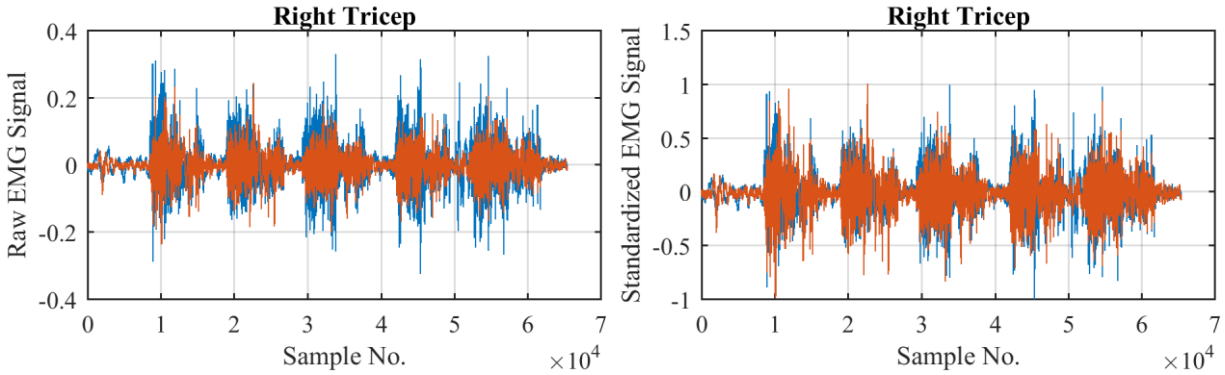

Figure 7. (a) Raw signal example; (b) Standardized signal example. (Blue = conventional; Orange = wearable)

2. Data Segmentation

Before extracting features from the EMG signals, we carried out data segmentation methods which are often used in real-time applications. In order to evaluate the similarity between the two sEMG signal types, two variations of data segmentation methods were both used in the current study: the disjoint window method (Figure 9) and the overlapping window method (Figure 8).[34,35] The length of 250 ms was chosen for the disjoint segmentation method; similarly, the length of 250 ms with 50 ms overlapping windows was selected for the overlapping segmentation method.

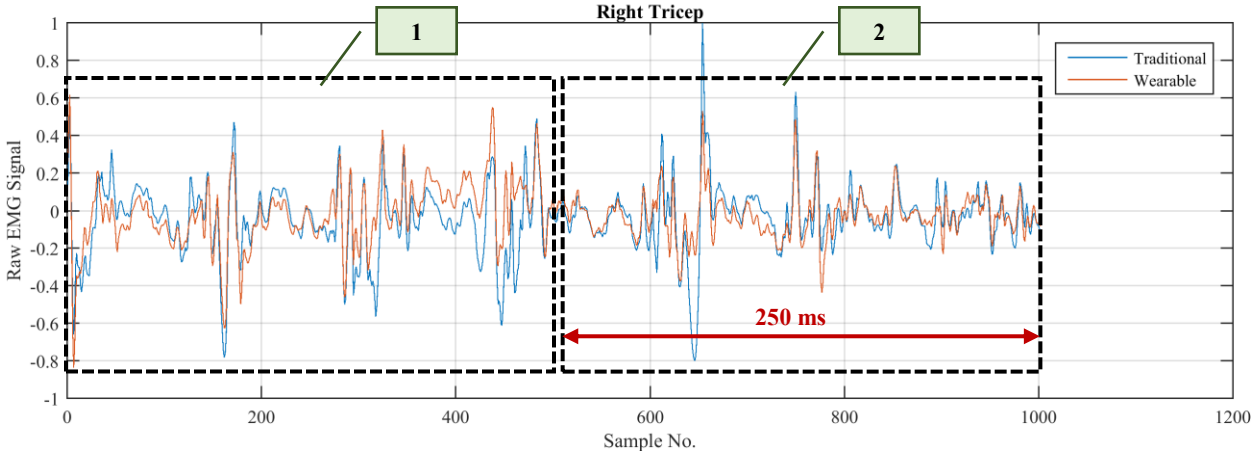

Figure 8. Disjoint segmentation method

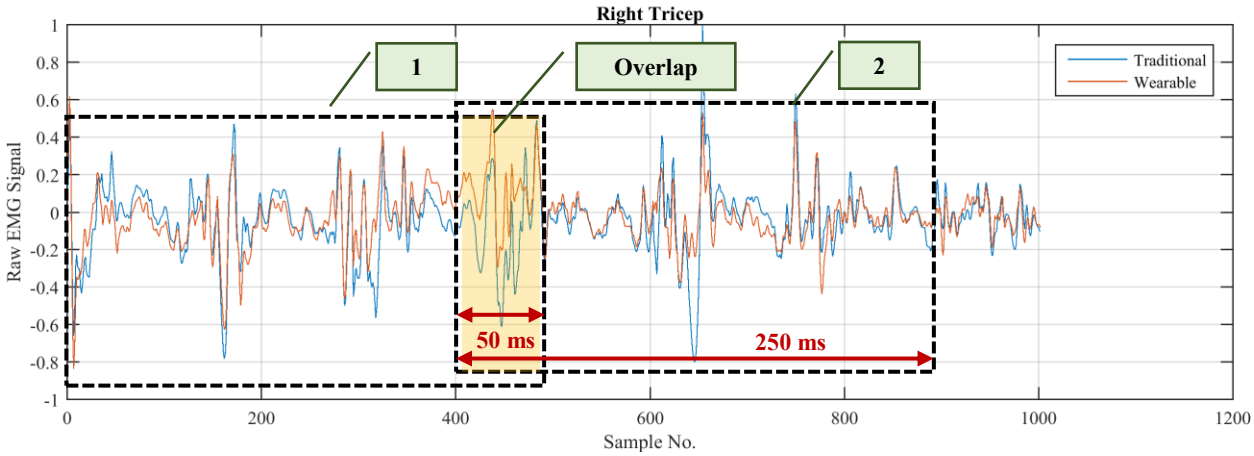

Figure 9. Overlapping segmentation method

3. sEMG Signal Features

In order to compare the two types of sEMG signals, eleven time-domain features that are commonly used for EMG pattern recognition were extracted in this study as the following:[36]

① Integrated absolute value of EMG (IEMG) is the summation of all rectified EMG signal values defined as

$$\mathrm{IEMG} = \sum_{k=1}^{N} |emg_k|$$

Where emg_k is the k^{th} sample and N is the number of samples in each segment window.

② Mean absolute value (MAV) of signal is the average of IEMG in a given segment window (often used in proportional control of prosthetic devices):[37]

$$\mathrm{MAV} = \frac{1}{\mathrm{N}} \sum_{k=1}^{N} |emg_k|$$

③ Root-mean-squared (RMS) method is another way to assess the intensity of signals in a given segment window:

$$\mathrm{RMS} = \frac{1}{\mathrm{N}} \sqrt{\sum_{k=1}^{N} emg_k^2}$$

④ Wave length (WL) of signal estimates the length of the waveform in a segment window:

$$\mathrm{WL} = \sum_{k=1}^{N-1} |emg_{k+1} - emg_k|$$

⑤ Difference absolute mean value (DAMV) of signal is the average of WL:

$$\mathrm{DAMV} = \frac{1}{\mathrm{N}-1} \sum_{k=1}^{N-1} |emg_{k+1} - emg_k|$$

⑥ Variance (VAR) of signal is a measure of the signal power:

$$\mathrm{VAR} = \frac{1}{\mathrm{N}-1} \sum_{k=1}^{N} emg_k^2$$

⑦ Zero crossings (ZC) of signal counts the number of times that the signal passes through the zero-point of the signal amplitude in a given window size of N:[38]

$$\mathrm{ZC} = \sum_{k=1}^{N} sgn(-emg_k \times emg_{k+1})$$

where

$$sgn(x) = \begin{cases} 1, if\ x > 0 \\ 0, otherwise. \end{cases}$$

⑧ Wilson amplitude (WAMP) of signal in a given window shows the number of times that each of the differences between two consecutive EMG signal values is larger than a particular threshold (set to 0.05 mV):[39]

$$\mathrm{WAMP} = \sum_{k=1}^{N} f(|emg_k - emg_{k+1}|)$$

where

$$f(x) = \begin{cases} 1, & if\ x > threshold \\ 0, & otherwise. \end{cases}$$

⑨ Slope sign change (SSC) is the count of the number of times the slope of the time-domain EMG signal changes the sign (positive or negative) in a given window, which can also be used as a frequency measurement:

$$\mathrm{SSC} = \sum_{k=1}^{N} f(emg_k - emg_{k-1}) \times (emg_k - emg_{k+1})$$

where

$$f(x) = \begin{cases} 1, & if\ x > 0 \\ 0, & otherwise. \end{cases}$$

⑩ Autoregressive (AR) models treat each sample of the EMG signal as a linear combination of previous samples plus an independent error term, with the assumption that the quasi-random nature of the EMG signals can be considered a Gaussian process.[40–42] For each k^{th} signal of EMG, the AR model is defined as

$$emg_k = -\sum_{j=1}^{q} a_j\, x_{(k-j)} + e_k$$

where emg_k denotes the recorded EMG signal, a_j denotes the AR coefficient, e_k denotes the residual white noise, and q denotes AR model's order (q=7, in this study). For analysis, the AR-coefficients were calculated by obtaining the least-squares of the forward and backward prediction errors while fitting a 7th-order AR model to emg_k. With q=7, there were 7 coefficients derived per emg_k, which were averaged (mean of AR-coefficients).

⑪ Together with the mean of AR model coefficients, RMS of (7th order) AR-coefficients were also calculated as another representation of the signal within a given segmentation window.

IV. Results

Pearson product-moment correlation coefficients, t-tests, and Bland-Altman tests were used to compare the two signal types. (The Bland-Altman method graphically compares two measurement techniques, by plotting their differences against the averages of the two, with one overlaying horizontal line at the mean difference and two overlaying lines at the limits of agreement which are ±1.96 times the standard deviation of the differences.)[43] As stated earlier, eleven features were extracted from the signals obtained from Conventional and Wearable EMG electrode condiions. The differences between their features were compared and examined using the aforementioned statistical analyses for each of the non-windowing, disjoint windowing, and overlapping windowing methods.

A. Trial Assessments (Non-segmentation Method)

In this non-segmentation analysis, all EMG signal features were extracted for the entire duration of each trial. The comparison results for the Left Biceps, Right Biceps, Left Triceps, and Right Triceps signals are displayed in Table 1, Table 2, Table 3, and Table 4, respectively. In these tables, the absolute errors between the conventional and wearable configurations (for each of the 11 features) were calculated, and then the average and standard deviation of these absolute errors were also computed. Moreover, to evaluate the differences between the two channels, the paired t-tests and the Bland-Altman tests have been employed as well. (Example Bland-Altman plots for the WL parameter for Biceps and Triceps muscles are shown in Figure 10.)

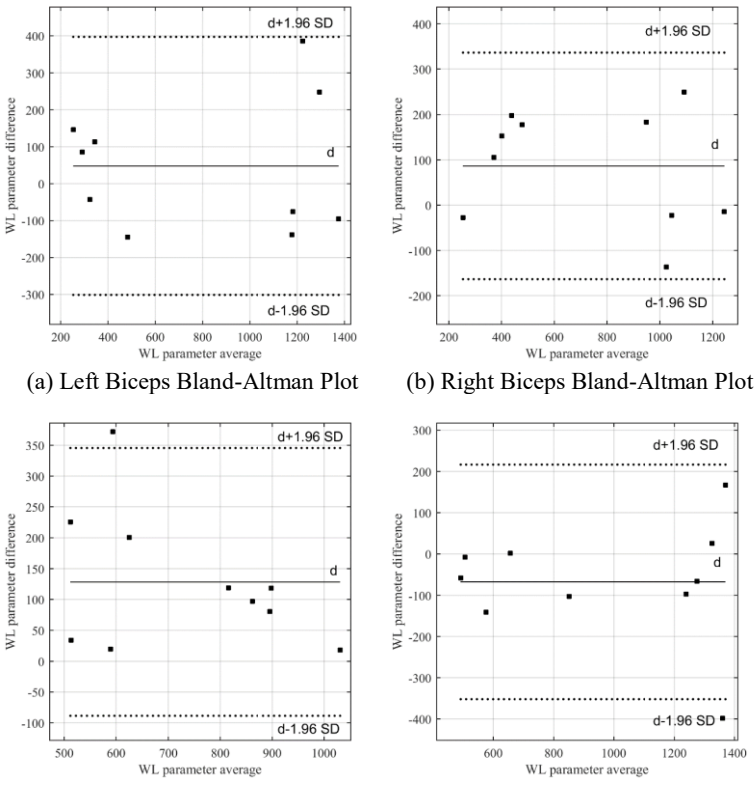

(a) Left Biceps Bland-Altman Plot (b) Right Biceps Bland-Altman Plot

(c) Left Triceps Bland-Altman Plot (d) Right Triceps Bland-Altman Plot

Figure 10. Bland-Altman plot examples of WL parameter

As reported in Table 1 through Table 4, the t-test results show that there are no significant differences between the conventional and wearable configurations for the four muscles in the majority of the features obtained. Left Biceps showed non-significant differences in all features; the WAMP feature difference was significant between the conventional and wearable settings for the Right Biceps muscle; DAMV differed between the conventional and wearable signal sources for the Left Triceps; and RMS of AR-coefficients differed for both Left and Right Triceps. However, given the extensiveness of these feature comparisons, these few statistical differences are relatively insignificant overall.

Table 1. The t-test results and Bland-Altman parameters for the features extracted from Left Biceps signals collected with conventional vs. wearable electrodes. (N.S. = non-significant)

Left Biceps								
	Feature Average		Absolute Error Value		T-test result (α=0.05)	Bland-Altman Plot Parameters		
	Conventional Electrodes	Wearable Electrodes	Mean	SD		Mean	Mean +1.96SD	Mean -1.96SD
IEMG	7560.90	7410.50	398.51	438.13	N.S.	150.43	1298.80	-997.92
MAV	1.93E-01	1.89E-01	8.56E-03	7.63E-03	N.S.	3.74E-03	2.56E-02	-1.81E-02
RMS	1.15E-03	1.11E-03	8.71E-05	5.39E-05	N.S.	3.63E-05	2.31E-04	-1.58E-04
WL	819.85	771.26	147.70	100.72	N.S.	48.59	397.90	-300.71
DAMV	1.75E-02	1.63E-02	3.46E-03	1.87E-03	N.S.	1.21E-03	8.85E-03	-6.43E-03
VAR	5.50E-02	5.28E-02	6.91E-03	3.70E-03	N.S.	2.18E-03	1.76E-02	-1.32E-02
ZC	1387.80	1327.40	163.40	151.24	N.S.	60.40	491.98	-371.18
WAMP	4154.80	4042.10	2588.90	817.66	N.S.	112.70	5691.50	-5466.10
SSC	8.65E+07	9.59E+07	9.35E+06	4.51E+06	N.S.	-9.35E+06	-5.09E+05	-1.82E+07
AR coeffs. Mean	3.37E-03	2.74E-03	6.87E-04	8.13E-04	N.S.	6.21E-04	2.32E-03	-1.08E-03
AR coeffs. RMS	9.19E-01	9.00E-01	3.14E-02	2.83E-02	N.S.	1.88E-02	9.48E-02	-5.72E-02

Table 2. The t-test results and Bland-Altman parameters for the features extracted from Right Biceps signals collected with conventional vs. wearable electrodes. (N.S. = non-significant)

Right Biceps								
	Feature Average		Absolute Error Value		T-test result (α=0.05)	Bland-Altman Plot Parameters		
	Conventional Electrodes	Wearable Electrodes	Mean	SD		Mean	Mean +1.96SD	Mean -1.96SD
IEMG	5389.60	5141.20	565.20	254.50	N.S.	248.39	1409.90	-913.08
MAV	1.22E-01	1.13E-01	1.48E-02	9.50E-03	N.S.	9.27E-03	3.96E-02	-2.10E-02
RMS	8.27E-04	7.30E-04	1.36E-04	1.02E-04	N.S.	9.68E-05	3.77E-04	-1.83E-04
WL	773.86	686.93	126.90	82.37	N.S.	86.93	337.02	-163.16
DAMV	1.73E-02	1.49E-02	3.28E-03	2.15E-03	N.S.	2.44E-03	8.62E-03	-3.75E-03
VAR	2.83E-02	2.33E-02	8.23E-03	5.08E-03	N.S.	4.92E-03	2.18E-02	-1.20E-02
ZC	1491.90	1414.40	129.90	91.43	N.S.	77.50	357.69	-202.69
WAMP	5896.40	4171.70	1724.70	664.08	$p < 0.05$	1724.70	3026.30	423.10
SSC	7.61E+07	8.05E+07	8.26E+06	2.89E+06	N.S.	-4.46E+06	1.10E+07	-1.99E+07
AR coeffs. Mean	3.31E-03	3.37E-03	8.94E-04	7.06E-04	N.S.	-6.13E-05	2.24E-03	-2.37E-03
AR coeffs. RMS	9.52E-01	9.34E-01	4.12E-02	3.44E-02	N.S.	1.79E-02	1.20E-01	-8.42E-02

Table 3. The t-test results and Bland-Altman parameters for the features extracted from Left Triceps signals collected with conventional vs. wearable electrodes. (N.S. = non-significant)

Left Triceps								
	Feature Average		Absolute Error Value		T-test result (α=0.05)	Bland-Altman Plot Parameters		
	Conventional Electrodes	Wearable Electrodes	Mean	SD		Mean	Mean +1.96SD	Mean -1.96SD
IEMG	613.30	7974.50	754.72	621.82	N.S.	638.85	2113.50	-835.82
MAV	1.89E-01	1.77E-01	1.55E-02	1.05E-02	N.S.	1.17E-02	4.11E-02	-1.77E-02
RMS	1.10E-03	9.98E-04	1.32E-04	7.99E-05	N.S.	1.00E-04	3.36E-04	-1.36E-04
WL	798.14	669.40	128.73	110.73	N.S.	128.73	345.76	-88.29
DAMV	1.81E-02	1.49E-02	3.25E-03	3.34E-03	$p < 0.05$	3.25E-03	9.80E-03	-3.30E-03
VAR	5.45E-02	4.54E-02	1.16E-02	6.35E-03	N.S.	9.06E-03	2.84E-02	-1.03E-02
ZC	1029.30	844.80	212.10	149.26	N.S.	184.50	548.24	-179.24
WAMP	2028.00	3187.70	1219.50	1256.50	N.S.	-1159.70	1423.40	-3742.80
SSC	8.62E+07	1.17E+08	3.10E+07	3.03E+07	N.S.	-3.10E+07	2.84E+07	-9.05E+07
AR coeffs. Mean	1.37E-03	1.42E-03	5.03E-04	4.12E-04	N.S.	-4.74E-05	1.26E-03	-1.36E-03
AR coeffs. RMS	1.13E+00	9.74E-01	1.56E-01	5.04E-02	$p < 0.05$	1.56E-01	2.55E-01	5.72E-02

Table 4. The t-test results and Bland-Altman parameters for the features extracted from Right Triceps signals collected with conventional vs. wearable electrodes. (N.S. = non-significant)

Right Triceps								
	Feature Average		Absolute Error Value		T-test result (α=0.05)	Bland-Altman Plot Parameters		
	Conventional Electrodes	Wearable Electrodes	Mean	SD		Mean	Mean +1.96SD	Mean -1.96SD
IEMG	5749.40	5782.20	485.51	373.66	N.S.	-32.82	1207.30	-1273.00
MAV	1.36E-01	1.34E-01	1.10E-02	6.89E-03	N.S.	1.74E-03	2.79E-02	-2.44E-02
RMS	9.00E-04	9.07E-04	7.26E-05	5.68E-05	N.S.	-6.65E-06	1.80E-04	-1.93E-04
WL	932.27	999.51	106.47	116.02	N.S.	-67.24	217.00	-351.48
DAMV	2.09E-02	2.26E-02	2.31E-03	2.13E-03	N.S.	-1.64E-03	3.72E-03	-7.01E-03
VAR	3.19E-02	3.25E-02	5.17E-03	3.94E-03	N.S.	-5.44E-04	1.26E-02	-1.37E-02
ZC	1817.40	2064.30	301.50	268.06	N.S.	-246.90	388.59	-882.39
WAMP	2586.20	1549.90	1036.30	355.01	N.S.	1036.30	1732.10	340.48
SSC	9.89E+07	1.42E+08	4.26E+07	3.49E+07	N.S.	-4.26E+07	2.59E+07	-1.11E+08
AR coeffs. Mean	3.25E-03	3.38E-03	4.85E-04	5.88E-04	N.S.	-1.28E-04	1.38E-03	-1.63E-03
AR coeffs. RMS	1.08E+00	9.69E-01	1.13E-01	3.93E-02	$p < 0.05$	1.13E-01	1.90E-01	3.58E-02

B. Overlapping Segmentation Method

As stated before, in the overlapping segmentation analysis, the signals were segmented into 250 ms windows with 50 ms overlapping periods and the EMG features were extracted from the segment windows. Totals of 1121, 1120, 1060, and 1060 windows were extracted from Right Triceps, Left Triceps, Right Biceps, and Left Biceps signals respectively. For assessing the similarities and differences between the conventional and wearable configurations, correlation coefficients between the conventional and wearable EMG signals were also calculated for each of the features with the combined 4361 windows (1121+1120+1060+1060 windows). As represented in Table 5, the paired t-test results (α=0.05) indicate non-significant differences between the two different EMG signal collection types.

Table 5. The obtained t-test results (α=0.05) and correlation coefficients comparing the conventional and wearable sEMG signals, for each muscle measured, using the overlapping segmentation method.

Parameter	Right Triceps (1121)		Left Triceps (1120)		Right Biceps (1060)		Left Biceps (1060)		Average Pearson's *r* (4361)
	Pearson's *r*	T-test result (α=0.05)	Pearson's *r*	T-test result (α=0.05)	Pearson's *r*	T-test result (α=0.05)	Pearson's *r*	T-test result (α=0.05)	
IEMG	0.85	N.S.	0.64	N.S.	0.77	N.S.	0.82	N.S.	0.77
MAV	0.85	N.S.	0.64	N.S.	0.77	N.S.	0.82	N.S.	0.77
RMS	0.88	N.S.	0.68	N.S.	0.83	N.S.	0.85	N.S.	0.81
WL	0.98	N.S.	0.96	N.S.	0.95	N.S.	0.92	N.S.	0.95
DAMV	0.85	N.S.	0.59	N.S.	0.81	N.S.	0.79	N.S.	0.76
VAR	0.98	N.S.	0.96	N.S.	0.95	N.S.	0.92	N.S.	0.95
ZC	0.74	N.S.	0.64	N.S.	0.84	N.S.	0.84	N.S.	0.77
WAMP	0.97	N.S.	0.93	N.S.	0.90	N.S.	0.84	N.S.	0.91
SSC	0.87	N.S.	0.86	N.S.	0.88	N.S.	0.90	N.S.	0.88
AR coeffs. Mean	0.73	N.S.	0.53	N.S.	0.81	N.S.	0.78	N.S.	0.71
AR coeffs. RMS	0.93	N.S.	0.94	N.S.	0.90	N.S.	0.92	N.S.	0.92

C. Disjoint Segmentation Method

Separate segments of 250 ms windows without overlap were used in the disjoint segmentation method. The results, shown in Table 6, are very similar to those from the overlapping segmentation method. Likewise, correlation coefficients and t-tests compared the two sEMG recording configurations.

Table 6. The obtained t-test results (α=0.05) and correlation coefficients comparing the conventional and wearable sEMG signals, for each muscle measured, using the disjoint segmentation method.

Parameter	Right Triceps (1121)		Left Triceps (1120)		Right Biceps (1060)		Left Biceps (1060)		Average Pearson's *r* (4361)
	Pearson's *r*	T-test result (α=0.05)	Pearson's *r*	T-test result (α=0.05)	Pearson's *r*	T-test result (α=0.05)	Pearson's *r*	T-test result (α=0.05)	
IEMG	0.84	N.S.	0.62	N.S.	0.76	N.S.	0.81	N.S.	0.76
MAV	0.84	N.S.	0.62	N.S.	0.76	N.S.	0.81	N.S.	0.76
RMS	0.87	N.S.	0.66	N.S.	0.83	N.S.	0.85	N.S.	0.80
WL	0.98	N.S.	0.96	N.S.	0.95	N.S.	0.92	N.S.	0.95
DAMV	0.85	N.S.	0.57	N.S.	0.81	N.S.	0.79	N.S.	0.75
VAR	0.98	N.S.	0.96	N.S.	0.95	N.S.	0.92	N.S.	0.95
ZC	0.73	N.S.	0.63	N.S.	0.84	N.S.	0.84	N.S.	0.76
WAMP	0.97	N.S.	0.93	N.S.	0.89	N.S.	0.85	N.S.	0.91
SSC	0.86	N.S.	0.86	N.S.	0.87	N.S.	0.89	N.S.	0.87
AR coeffs. Mean	0.74	N.S.	0.55	N.S.	0.81	N.S.	0.78	N.S.	0.72
AR coeffs. RMS	0.93	N.S.	0.94	N.S.	0.90	N.S.	0.92	N.S.	0.92

V. Discussion and Conclusion

In the present study, we have tested the validity of using an alternative sEMG collection method, which can be easily and inexpensively implemented in a cut-and-sew scale wearable constructions with widely accessible materials that can be adapted into many different system form factors. This wearable sEMG signal recording method of using dry metal snap electrodes with anti-slip medical wraps is especially designed to demonstrate the feasibility of obtaining biosignals to aid in biomechanical studies where the placement of conventional sensors are inhibited by small, thick, or rigid compartments surrounding the body. The unique dual-channel EMG electrode setup employed in this study allowed us to directly compare the quality of sEMG signals with extensive quantitative analyses, as the signals were concurrently collected on the same muscle for the same activities. In this study, these robust time domain feature comparisons have confirmed that this wearable method of sEMG measurement is largely similar to the conventional means of sEMG studies, both qualitatively and quantitatively. This outcome is especially encouraging, since there was a risk of having potentially collected two different qualities of signals due to the fact that both pairs of electrodes, having to share the real estate of the same muscle with the other pair, slightly deviated from the ideal location of the longitudinal centerline of the muscle belly.[23]

Even the few feature differences found between the two methods in some muscle activities (which may be due to a number of other factors such as crosstalk from other muscles and motion artifacts) are minor differences that can be corrected by with further signal processing such as moving average smoothing and low-pass filtering. The current validation study with 11 different time-domain EMG features extracted from 40 trials collected from four muscles, with three different signal analyses methods, shows strong evidence in the functional equivalence of the alternative dry, wearable, reusable electrode configuration to the conventional gelled, adhesive, disposable electrode setup. Our robust validation results from the segmentation approaches, in particular, show promise in using such soft-goods-based sEMG sensing interface for real-time applications, as segmentation is commonly used in real-time EMG-controlled systems. Our tests also showed high correlations between the vectors of features extracted from conventional and wearable sEMG signals.

Implications of the present study include contribution to an improved design of wearable biosignal collection systems, such as the previous work of intra-spacesuit sEMG collection garment for studying biomechanics of suited astronauts. Commensurate with the advances in the soft robotics research, such flexible sEMG collection interface, which can be easily constructed and adapted into garment-like form factors, may also be used in the future generation of flexible mobility assistive devices that are less time-comsuing for setup and more comfortable to users.

There yet remain many obstacles to designing a perfect wearable biosignal data collection system, however, as several limitations still need to be addressed in this current wearable electrode configuration. In sEMG recordings, the lead-electrode contact point is susceptible to motion artifacts from external disturbances, and the cable can pick up ambient noise in many circumstances; conversely, pre-amplification on or near the skin requires attachment of hardware on the body that adds bulk, which may also compromise flexibility, comfort, and usability in many circumstances. The currently introduced wearable sEMG collection method provides an alternative means to achieve a skin-electrode contact only, and clip leads still had to be secured with tapes in this study, in order to minimize the motion artifacts occurring at the cable-electrode contact area. Establishing a reliable connection between the electrodes and the amplifier device remains a difficult to be solved, hand-in-hand with the challenges in the e-textile interconnect methods.[44]

Future work includes further establishing the repeatability and consistency of such alternative electrode performances with repeated don/doff trials across more human subjects in various settings, validating the long-term usability and reliability of such wearable sEMG electrode configurations, and designing similarly appropriate wearable sensing interfaces for other muscles that may not be compatible with a simple elastic-band form factor, such as the shoulder muscles.[33] Also, metal snaps used in clothing and crafts, despite their prevalence, are usually made of nickel, which is not biocompatible and may cause allergic reactions in some individuals.[45] Advanced versions of such wearable sEMG collection interfaces should therefore find alternative electrode materials to be used on skin; manufacturing similar snap-like electrode components with Ag-AgCl may be ideal due to their functional superiority as on-skin electrodes.[27,28] Solving these challenges would get researchers and designers closer to the development of a user-friendly, comfortable, and flexible signal collection system that can be commercialized and be actively deployed outside laboratory environments.

Acknowledgements

This work was supported by the National Science Foundation under grant #1722738.

References

[1]Diaz, A., Anderson, A., Kracik, M., Trotti, G., and Hoffman, J., "Development of a comprehensive astronaut spacesuit injury database," *63rd International Astronautical Congress*, 2012, pp. 1–9.

[2]Strauss, S., Krog, R. L., and Feiveson, A. H., "Extravehicular mobility unit training and astronaut injuries," *Aviation Space and Environmental Medicine*, vol. 76, 2005, pp. 469–474.

[3]Scheuring, R. A., Mathers, C. H., Jones, J. A., and Wear, M. L., "Musculoskeletal injuries and minor trauma in space: Incidence and injury mechanisms in U.S. astronauts," *Aviation Space and Environmental Medicine*, vol. 80, 2009, pp. 117–124.

[4]Williams, D. R., and Johnson, B. J., "EMU Shoulder Injury Tiger Team Report," *NASA Technical Paper*, vol. 212058, 2003, pp. 1–90.

[5]Chen, B., Ma, H., Qin, L.-Y., Gao, F., Chan, K.-M., Law, S.-W., Qin, L., and Liao, W.-H., "Recent developments and challenges of lower extremity exoskeletons," *Journal of Orthopaedic Translation*, vol. 5, Apr. 2016, pp. 26–37.

[6]Maciejasz, P., Eschweiler, J., Gerlach-Hahn, K., Jansen-Troy, A., and Leonhardt, S., "A survey on robotic devices for upper limb rehabilitation," *Journal of NeuroEngineering and Rehabilitation*, vol. 11, 2014, pp. 1–29.

[7]Yap, H. K., Lim, J. H., Nasrallah, F., Goh, J. C. H., and Yeow, R. C. H., "A soft exoskeleton for hand assistive and rehabilitation application using pneumatic actuators with variable stiffness," *Proceedings - IEEE International Conference on Robotics and Automation*, vol. 2015-June, 2015, pp. 4967–4972.

[8]Meng, Q., Xiang, S., and Yu, H., "Soft Robotic Hand Exoskeleton Systems: Review and Challenges Surrounding the Technology," vol. 86, 2017, pp. 186–190.

[9]Asbeck, A. T., Dyer, R. J., Larusson, A. F., and Walsh, C. J., "Biologically-inspired soft exosuit," *IEEE International Conference on Rehabilitation Robotics*, 2013, pp. 1–8.

[10]Caldwell, D. G., Tsugarakis, N. G., Kousidou, S., Costa, N., and Sarakoglou, I., "'Soft' Exoskeletons for Upper and Lower Body Rehabilitation - Design, Control and Testing," *International Journal of Humanoid Robotics*, vol. 4, 2007, pp. 1–24.

[11]Koh, T. H., Cheng, N., Yap, H. K., and Yeow, C. H., "Design of a soft robotic elbow sleeve with passive and intent-controlled actuation," *Frontiers in Neuroscience*, vol. 11, 2017, pp. 1–12.

[12]Fleischer, C., Wege, A., Kondak, K., and Hommel, G., "Application of EMG signals for controlling exoskeleton robots," *Biomedizinische Technik*, vol. 51, 2006, pp. 314–319.

[13]Peternel, L., Noda, T., Petrič, T., Ude, A., Morimoto, J., and Babič, J., "Adaptive control of exoskeleton robots for periodic assistive behaviours based on EMG feedback minimisation," *PLoS ONE*, vol. 11, 2016, pp. 1–26.

[14]Lenzi, T., De Rossi, S. M. M., Vitiello, N., and Carrozza, M. C., "Intention-based EMG control for powered exoskeletons," *IEEE Transactions on Biomedical Engineering*, vol. 59, 2012, pp. 2180–2190.

[15]Buchanan, T. S., Lloyd, D. G., Manal, K., and Besier, T. F., "Neuromusculoskeletal Modeling: Estimation of Muscle Forces and Joint Moments and Movements From Measurements of Neural Command," *Journal of applied biomechanics*, vol. 20, Nov. 2004, pp. 367–395.

[16]Paradiso, R., Caldani, L., and Pacelli, M., "Knitted Electronic Textiles," *Wearable Sensors: Fundamentals, Implementation and Applications*, vol. 1, 2014, pp. 153–174.

[17]Clancy, E. A., Morin, E. L., and Merletti, R., "Sampling, noise-reduction and amplitude estimation issues in surface electromyography," *Journal of Electromyography and Kinesiology*, vol. 12, 2002, pp. 1–16.

[18]Day, S., *Important Factors in Surface EMG Measurement*, Calgary, AB: 2002.

[19]Bergmann, J. H. M., and McGregor, A. H., "Body-worn sensor design: What do patients and clinicians want?," *Annals of Biomedical Engineering*, vol. 39, 2011, pp. 2299–2312.

[20]Hamilton, N., Weimar, W., and Luttgens, K., *Kinesiology: Scientific basis of human motion*, New York, NY: McGraw-Hill, 2012.

[21]Baker, R., and Shortland, A., "Electromyography," *Measuring Walking: A Handbook of Clinical Gait Analysis*, R. Baker, ed., London: Mac Keith Press, 2013, pp. 71–87.

[22]Jamal, M. Z., "Signal Acquisition Using Surface EMG and Circuit Design Considerations for Robotic Prosthesis," *Computational Intelligence in Electromyography Analysis - A Perspective on Current Applications and Future Challenges*, InTech, 2012.

[23]De Luca, C. J., *Surface Electromyography: Detection and Recording*, 2002.

[24]Konrad, P., *The ABC of EMG: A Practical Introduction to Kinesiological Electromyography*, 2005.

[25]Cömert, A., Honkala, M., and Hyttinen, J., "Effect of pressure and padding on motion artifact of textile electrodes," *BioMedical Engineering Online*, vol. 12, 2013.

[26]Medrano, G., Ubl, A., Zimmermann, N., Gries, T., and Leonhardt, S., "Skin Electrode Impedance of Textile Electrodes for Bioimpedance Spectroscopy," *13th International Conference on Electrical Bioimpedance and the 8th Conference on Electrical Impedance Tomography*, H. Scharfetter and R. Merwa, eds., Berlin, Heidelberg: Springer Berlin Heidelberg, 2007, pp. 260–263.

[27]Tallgren, P., Vanhatalo, S., Kaila, K., and Voipio, J., "Evaluation of commercially available electrodes and gels for recording of slow EEG potentials," *Clinical Neurophysiology*, vol. 116, 2005, pp. 799–806.

[28]Albulbul, A., "Evaluating Major Electrode Types for Idle Biological Signal Measurements for Modern Medical Technology," *Bioengineering*, vol. 3, 2016, pp. 20–20.

[29]Paleos, G. A., *What are hydrogels?*, Butler, PA: Pittsburgh Plastics Manufacturing Inc., 2012.

[30]Jossinet, J., and McAdams, E., "Hydrogel electrodes in biosignal recording," *Proceedings of the Annual Conference on Engineering in Medicine and Biology*, vol. 12, 1990, pp. 1490–1491.

[31]Chirani, N., Yahia, L., Gritsch, L., Motta, F. L., Chirani, S., and Faré, S., "History and Applications of Hydrogels," *Journal of Biomedical Sciences*, vol. 4, Oct. 2015.

[32]Roy, S. H., De Luca, G., Cheng, M. S., Johansson, A., Gilmore, L. D., and De Luca, C. J., "Electro-mechanical stability of surface EMG sensors," *Medical & Biological Engineering & Computing*, vol. 45, May 2007, pp. 447–457.

[33]Lee, J. W., Wang, S., Albers, C., and Dunne, L. E., "Garment-based EMG System for Intra-spacesuit Biomechanics Analysis," *2018 ACM International Symposium on Wearable Computers (ISWC '18)*, 2018.

[34]Tenore, F. V. G., Ramos, A., Fahmy, A., Acharya, S., Etienne-Cummings, R., and Thakor, N. V., "Decoding of Individuated Finger Movements Using Surface Electromyography," *IEEE Transactions on Biomedical Engineering*, vol. 56, May 2009, pp. 1427–1434.

[35]Huang, Y., Englehart, and K. B., Hudgins, B., and Chan, A. D. C., "A Gaussian mixture model based classification scheme for myoelectric control of powered upper limb prostheses," *IEEE Transactions on Biomedical Engineering*, vol. 52, Nov. 2005, pp. 1801–1811.

[36]Mokhlesabadifarahani, B., and Gunjan, V. K., *EMG Signals Characterization in Three States of Contraction by Fuzzy Network and Feature Extraction*, Singapore: Springer Singapore, 2015.

[37]Phinyomark, A., Hirunviriya, S., Limsakul, C., and Phukpattaranont, P., "Evaluation of EMG feature extraction for hand movement recognition based on Euclidean distance and standard deviation," *ECTI-CON2010: The 2010 ECTI International Confernce on Electrical Engineering/Electronics, Computer, Telecommunications and Information Technology*, 2010, pp. 856–860.

[38]Chang, G.-C., Kang, W.-J., Luh, J.-J., Cheng, C.-K., Lai, J.-S., Chen, J.-J. J., and Kuo, T.-S., "Real-time implementation of electromyogram pattern recognition as a control command of man-machine interface," *Medical Engineering & Physics*, vol. 18, Oct. 1996, pp. 529–537.

[39]Sang-Hui Park, and Seok-Pil Lee, "EMG pattern recognition based on artificial intelligence techniques," *IEEE Transactions on Rehabilitation Engineering*, vol. 6, Dec. 1998, pp. 400–405.

[40]Paiss, O., and Inbar, G. F., "Autoregressive Modeling of Surface EMG and Its Spectrum with Application to Fatigue," *IEEE Transactions on Biomedical Engineering*, vol. BME-34, Oct. 1987, pp. 761–770.

[41]Liu, X., Zhou, R., Yang, L., and Li, G., "Performance of various EMG features in identifying ARM movements for control of multifunctional prostheses," *Computing and Telecommunication 2009 IEEE Youth Conference on Information*, 2009, pp. 287–290.

[42]Tomaszewski, J., Amaral, T. G., Dias, O. P., Wołczowski, A., and Kurzyński, M., "EMG signal classification using neural network with AR model coefficients," *IFAC Proceedings Volumes*, vol. 42, 2009, pp. 318–325.

[43]Tarvirdizadeh, B., Golgouneh, A., Khodabakhshi, E., and Tajdari, F., "An assessment of a similarity between the right and left hand photoplethysmography signals, using time and frequency features of heart-rate-variability signal," *2017 IEEE 4th International Conference on Knowledge-Based Engineering and Innovation (KBEI)*, Tehran: IEEE, 2017, pp. 0588–0594.

[44]Islam Molla, Md. T., Goodman, S., Schleif, N., Berglund, M. E., Zacharias, C., Compton, C., and Dunne, L. E., "Surface-mount manufacturing for e-textile circuits," *Proceedings of the 2017 ACM International Symposium on Wearable Computers - ISWC '17*, 2017, pp. 18–25.

[45]Silverberg, N. B., Licht, J., Friedler, S., Sethi, S., and Laude, T. A., "Nickel contact hypersensitivity in children," *Pediatric Dermatology*, vol. 19, 2002, pp. 110–113.